

Valence Tautomerism in a High-Valent Manganese–Oxo Porphyrinoid Complex Induced by a Lewis Acid

Panee Leeladee,[†] Regina A. Baglia,[†] Katharine A. Prokop,[†] Reza Latifi,^{‡,§} Sam P. de Visser,^{*,‡} and David P. Goldberg^{*,†}

[†]Department of Chemistry, The Johns Hopkins University, 3400 North Charles Street, Baltimore, Maryland 21218, United States

[‡]The Manchester Interdisciplinary Biocentre and School of Chemical Engineering and Analytical Science, The University of Manchester, 131 Princess Street, Manchester M1 7DN, United Kingdom

S Supporting Information

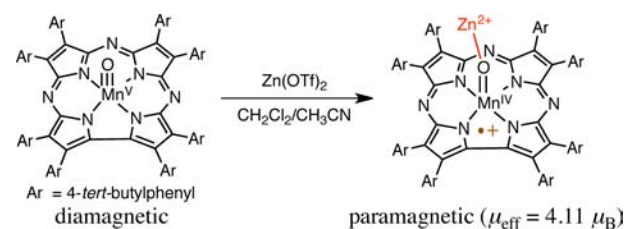
ABSTRACT: Addition of the Lewis acid Zn^{2+} to $(\text{TBP}_8\text{Cz})\text{Mn}^{\text{V}}(\text{O})$ induces valence tautomerization, resulting in the formation of $[(\text{TBP}_8\text{Cz}^{\bullet+})\text{Mn}^{\text{IV}}(\text{O})-\text{Zn}^{2+}]$. This new species was characterized by UV–vis, EPR, the Evans method, and ^1H NMR and supported by DFT calculations. Removal of Zn^{2+} quantitatively restores the starting material. Electron-transfer and hydrogen-atom-transfer reactions are strongly influenced by the presence of Zn^{2+} .

Redox-inactive metal ions serving as Lewis acids have recently come under scrutiny for their potential influence on the reactivity of biologically relevant transition metal centers. The influence of redox-inactive metal ions on high-valent Mn–oxo species is of particular importance because of the high-resolution X-ray structure of the oxygen-evolving complex of photosystem II, which revealed a Lewis acidic Ca^{2+} ion intimately associated with the catalytic center in an Mn_4CaO_5 cluster.¹ Although mechanistic speculations suggest that the Ca^{2+} ion may interact directly with high-valent Mn–O species during the water oxidation process,² the role of this redox-inactive metal ion has yet to be clarified. In regard to the reactivity of Mn complexes with Lewis acids, an early study from Collins³ provided the first and only example of the influence of redox-inactive metal ions on an isolable $\text{Mn}^{\text{V}}(\text{O})$ compound, revealing enhanced reactivity of the $\text{Mn}^{\text{V}}(\text{O})$ complex toward oxygen atom transfer (OAT). In this case the Lewis acids did not bind directly to the oxo ligand but rather to a secondary site incorporated in the tetraamide ligand. A dramatic acceleration in rates of oxidation of alkanes by addition of Lewis acids to MnO_4^- was demonstrated by Lau⁴ and others.⁵ More recently, Borovik reported that the rates of O_2 reduction by a Mn^{II} complex were accelerated by group 2 metal ions.⁶ In related work, Fukuzumi and Nam provided some fundamental insights regarding the influence of Lewis acids on the electron-transfer (ET) and OAT reactivity of high-valent non-heme iron–oxo complexes.⁷ An interesting example of a Cu^{2+} ion interacting with a $\text{Cr}^{\text{V}}(\text{O})$ corrole was also described.⁸ With the exception of the few former reports, much remains unknown about the reactivity of biologically relevant metal–oxo complexes with Lewis acids.

Herein we describe the influence of redox-inactive metal ions on an isolable $\text{Mn}^{\text{V}}(\text{O})$ complex, $(\text{TBP}_8\text{Cz})\text{Mn}^{\text{V}}(\text{O})$ (TBP_8Cz

= octakis(*p*-*tert*-butylphenyl)corrolazinato(3–)). We find that Zn^{2+} binds to the $\text{Mn}^{\text{V}}(\text{O})$ complex with high affinity and induces interconversion of this complex to a valence tautomer characterized as a $\text{Mn}^{\text{IV}}(\text{O})$ π -cation-radical (Scheme 1).

Scheme 1



Moreover, it is demonstrated that this chemically driven valence tautomerization is fully reversible and that the presence of the Lewis acidic Zn^{2+} ion has a dramatic effect on its ET and formal hydrogen-atom-transfer (HAT) reactivity.

Addition of $\text{Zn}(\text{OTf})_2$ (1 equiv in 20 μL of CH_3CN) to a solution of $(\text{TBP}_8\text{Cz})\text{Mn}^{\text{V}}(\text{O})$ (16 μM) in CH_2Cl_2 at 23 $^\circ\text{C}$ resulted in a gradual color change over 1 h from bright green to brown. Monitoring this reaction by UV–vis spectroscopy revealed isosbestic conversion of the $\text{Mn}^{\text{V}}(\text{O})$ complex (λ_{max} , nm (ϵ $\text{M}^{-1} \text{cm}^{-1}$): 419 (6.29×10^4), 634 (1.99×10^4)) to a new spectrum with peaks at 419 (3.97×10^4) and 789 (7.75×10^3) nm (Figure 1). Addition of excess Zn^{2+} (1–20 equiv) led to no further change in the UV–vis, and the final spectrum ($\lambda_{\text{max}} = 789$ nm) with 20 equiv of Zn^{2+} was stable at room temperature. The decrease and broadening of the Soret band at 419 nm, the loss of the Q-band at 634 nm, and the appearance of a weaker long-wavelength band at 789 nm are characteristic of the formation of a porphyrin or corrole π -cation radical.⁹ In a previous report, we showed that reaction of $(\text{TBP}_8\text{Cz})\text{Mn}^{\text{V}}(\text{O})$ with one-electron oxidants (e.g., $\text{Ar}_3\text{N}^{\bullet+}$) resulted in the production of a π -cation-radical complex $[(\text{TBP}_8\text{Cz}^{\bullet+})\text{Mn}^{\text{V}}(\text{O})]$, where the oxidizing equivalent mainly resides on the corrolazine ligand.¹⁰ The spectrum of the oxidized complex (410, 780 nm) is strikingly similar to that seen for the product in the $\text{Zn}(\text{OTf})_2$ reaction. These results suggested that addition of $\text{Zn}(\text{OTf})_2$ caused the one-electron oxidation of (TBP_8Cz) -

Received: May 11, 2012

Published: June 5, 2012

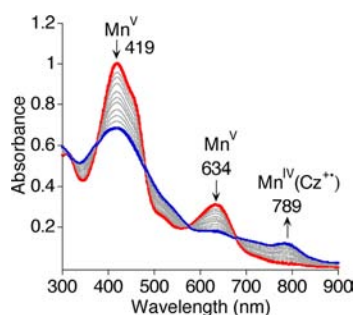


Figure 1. Time-resolved UV-vis spectra of $(\text{TBP}_8\text{Cz})\text{Mn}^{\text{V}}(\text{O}) + \text{Zn}(\text{OTf})_2$ (1 equiv) for 1 h at 23 °C in $\text{CH}_2\text{Cl}_2/\text{CH}_3\text{CN}$ (100:1 v:v).

$\text{Mn}^{\text{V}}(\text{O})$, but given that Zn^{2+} is redox-inactive, it was presumed that oxidation was a result of the aerobic reaction conditions. However, treatment of $(\text{TBP}_8\text{Cz})\text{Mn}^{\text{V}}(\text{O})$ with $\text{Zn}(\text{OTf})_2$ under strictly air-free conditions did not change the outcome of this reaction (Figure S2). Addition of excess NaOTf (100 equiv) to the $\text{Mn}^{\text{V}}(\text{O})$ complex also showed no change by UV-vis. This control experiment rules out coordination of OTf^- as the cause of the π -cation-radical formation and shows that the weaker Lewis acid Na^+ cannot substitute for Zn^{2+} .

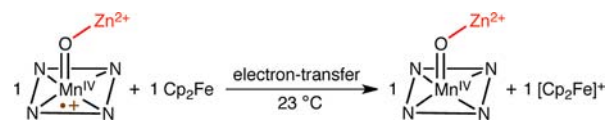
^1H NMR spectroscopy of $(\text{TBP}_8\text{Cz})\text{Mn}^{\text{V}}(\text{O}):\text{Zn}(\text{OTf})_2$ (1:2) in $\text{CD}_2\text{Cl}_2/\text{CD}_3\text{CN}$ revealed a paramagnetic spectrum (Figure S6), in stark contrast to the well-resolved diamagnetic spectrum seen for the starting low-spin d^2 $\text{Mn}^{\text{V}}(\text{O})$ complex. With Zn^{2+} -facilitated oxidation ruled out, the paramagnetic NMR spectrum and UV-vis data suggested to us that perhaps Zn^{2+} coordination induces the interconversion of $(\text{TBP}_8\text{Cz})\text{Mn}^{\text{V}}(\text{O})$ with a valence tautomer, in which an electron from the Cz ring is transferred to Mn to give the electronic isomer $[(\text{TBP}_8\text{Cz}^{\bullet+})\text{Mn}^{\text{IV}}(\text{O})-\text{Zn}^{2+}]$. Valence tautomerization is well documented in metalloporphyrins and metalcorroles¹¹ and has been proposed as playing a key role in the catalytic pathways of heme enzymes and porphyrin catalysts.^{11a}

The proposed valence tautomer can be expected to exhibit a paramagnetic ground state, with a high-spin Mn^{IV} ($S = 3/2$) ion either antiferromagnetically ($S_{\text{total}} = 1$) or ferromagnetically ($S_{\text{total}} = 2$) coupled to a Cz-based radical. An Evans method measurement gives $\mu_{\text{eff}} = 4.11 \mu_{\text{B}}$, which falls between those predicted for $S = 1$ ($2.83 \mu_{\text{B}}$) and $S = 2$ ($4.90 \mu_{\text{B}}$). In fact, $4.11 \mu_{\text{B}}$ is also quite close to the value predicted for non-interacting $h_s\text{-Mn}^{\text{IV}}$ and $\text{Cz}^{\bullet+}$ centers ($4.24 \mu_{\text{B}}$). For comparison, the nature and extent of the magnetic coupling in $\text{Mn}^{\text{III}}(\text{porph}^{\bullet+})$ complexes has led to conflicting interpretations that include both coupled and uncoupled descriptions.¹² X-band EPR spectroscopy of $[(\text{TBP}_8\text{Cz}^{\bullet+})\text{Mn}^{\text{IV}}(\text{O})-\text{Zn}^{2+}]$ at 77 K revealed that the compound was EPR silent, consistent with an integer-spin Mn^{IV} π -cation-radical complex. An unambiguous assignment of the coupling in $[(\text{TBP}_8\text{Cz}^{\bullet+})\text{Mn}^{\text{IV}}(\text{O})-\text{Zn}^{2+}]$ cannot be made at this time. However, taken together, the magnetic data provide strong evidence for the conclusion that a Mn^{IV} π -cation-radical complex is generated upon addition of Zn^{2+} ions.

The ET properties of $[(\text{TBP}_8\text{Cz}^{\bullet+})\text{Mn}^{\text{IV}}(\text{O})-\text{Zn}^{2+}]$ were next investigated, providing further insights into the nature of this species and revealing some novel ET behavior not seen previously for the $\text{Mn}^{\text{V}}(\text{O})$ starting material. The redox potential for the $\text{Mn}^{\text{V}}(\text{O})$ complex (0.02 V vs SCE)¹³ predicts that the driving force for one-electron reduction by ferrocene (Fc) (0.37 V vs SCE) is significantly uphill ($\Delta G_{\text{et}} = 0.35$ eV). Experimental verification of this prediction has been made, where no reaction is observed between $(\text{TBP}_8\text{Cz})\text{Mn}^{\text{V}}(\text{O})$ and

Fc, and only more strongly reducing Fc derivatives (e.g., $[\text{Fe}(\text{C}_5\text{HMe}_4)_2]$, $E_{\text{ox}} = -0.04$ V vs SCE) react with the $\text{Mn}^{\text{V}}(\text{O})$ complex ($k_{\text{et}} = (7.5 \pm 0.4) \times 10^4 \text{ M}^{-1} \text{ s}^{-1}$).¹⁴ In contrast, titration of a solution of $(\text{TBP}_8\text{Cz})\text{Mn}^{\text{V}}(\text{O}):\text{Zn}(\text{OTf})_2$ (1:20) with Fc leads to a rapid reaction, resulting in the characteristic spectrum for a Mn^{IV} complex and closed-shell Cz ring, $[(\text{TBP}_8\text{Cz})\text{Mn}^{\text{IV}}]^+$ (443, 724 nm)¹⁴ (Scheme 2). The

Scheme 2



stoichiometry of the ET reaction was confirmed to be 1:1 (Figure S9). Our previous attempts to reduce the $(\text{TBP}_8\text{Cz})\text{Mn}^{\text{V}}(\text{O})$ complex with Fc derivatives resulted in direct two-electron reduction to give $(\text{TBP}_8\text{Cz})\text{Mn}^{\text{III}}$, with no observable Mn^{IV} intermediate. The $[(\text{TBP}_8\text{Cz})\text{Mn}^{\text{IV}}]^+$ complex was only successfully characterized under oxidizing conditions, in which $(\text{Cz})\text{Mn}^{\text{III}}$ was treated with strong one-electron oxidants.¹⁴ The ET properties of the $[(\text{TBP}_8\text{Cz}^{\bullet+})\text{Mn}^{\text{IV}}(\text{O})-\text{Zn}^{2+}]$ complex are fully consistent with the valence tautomer assignment and indicate that $[(\text{TBP}_8\text{Cz}^{\bullet+})\text{Mn}^{\text{IV}}(\text{O})-\text{Zn}^{2+}]$ has a significantly higher redox potential than the starting Mn^{V} valence tautomer.

Efficient sequestration of the Zn^{2+} ions leads to regeneration of the starting $(\text{TBP}_8\text{Cz})\text{Mn}^{\text{V}}(\text{O})$ complex. Addition of excess 1,10-phenanthroline, a strong Zn^{2+} chelator, to a solution of $(\text{TBP}_8\text{Cz})\text{Mn}^{\text{V}}(\text{O}):\text{Zn}(\text{OTf})_2$ (1:1) caused the immediate reversion of the π -cation-radical spectrum back to that of the starting $\text{Mn}^{\text{V}}(\text{O})$ complex (Scheme 3, Figure 2a). Control

Scheme 3. Chelation of Zn^{2+} by 1,10-Phenanthroline (phen)

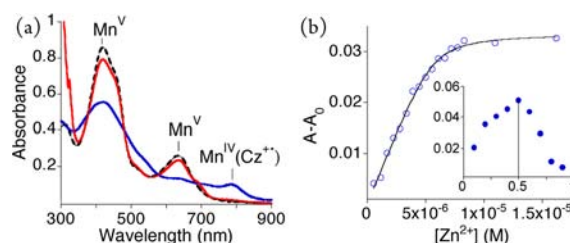
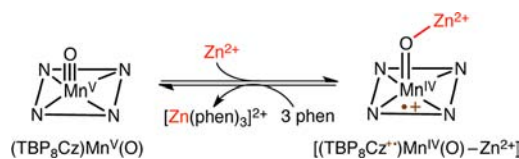


Figure 2. (a) UV-vis spectra of $(\text{TBP}_8\text{Cz})\text{Mn}^{\text{V}}(\text{O})$ (dashed line), $[(\text{TBP}_8\text{Cz}^{\bullet+})\text{Mn}^{\text{IV}}(\text{O})-\text{Zn}^{2+}]$ (blue line), and after addition of 1,10-phenanthroline (30 equiv) (red line). (b) Binding isotherm (plotted at 789 nm) for the addition of $\text{Zn}(\text{OTf})_2$. Inset: Job's plot ($x = [\text{Zn}^{2+}]/([\text{Zn}^{2+}] + [(\text{TBP}_8\text{Cz})\text{Mn}^{\text{V}}(\text{O})])$, $y = A - A_0$).

reactions performed by adding $[\text{Zn}(\text{phen})_3]^{2+}$ to $(\text{TBP}_8\text{Cz})\text{Mn}^{\text{V}}(\text{O})$ did not result in any change by UV-vis, confirming that “free” Zn^{2+} is required to bind $(\text{TBP}_8\text{Cz})\text{Mn}^{\text{V}}(\text{O})$ in order to observe the conversion. Spectral titration of $(\text{TBP}_8\text{Cz})\text{Mn}^{\text{V}}(\text{O})$ with $\text{Zn}(\text{OTf})_2$ results in a binding isotherm for Zn^{2+} , as shown in Figure 2b. This curve can be fit by a 1:1 binding model, which yields an association constant for Zn^{2+} of $K_a = 4.03 \times 10^6 \text{ M}^{-1}$. A Job's plot (Figure 2b, inset) reaches a

maximum at a molar ratio of 0.5, confirming a 1:1 binding stoichiometry. The relatively high K_a obtained from the binding curve indicates a surprisingly strong interaction between the $\text{Mn}^{\text{V}}(\text{O})$ complex and the Lewis acidic Zn^{2+} ion, but one which is fully reversible upon chelation with 1,10-phenanthroline.

The reversible interconversion of valence tautomers is a highly desirable feature for their potential use in electronic devices and other related applications. A well-known example of chemically driven valence tautomerization is the addition of strong axial donors (e.g., OR^-) to $\text{Mn}^{\text{III}}(\text{porph}^{+\bullet})$ complexes, which induces their conversion to $\text{Mn}^{\text{IV}}(\text{porph})$.^{11d} Mn-salen complexes have exhibited acid-dependent valence tautomerization.¹⁵ However, the reversibility of these processes has not been demonstrated. Metal complexes and redox-active ligands, including both non-porphyrin (e.g., quinonoid- M^{n+}) and porphyrin complexes, have exhibited reversible valence tautomer behavior, but these systems typically respond to temperature, pH, or pressure changes to control the interconversion.^{11b,16} The Zn^{2+} -induced interconversion described here is, to our knowledge, the first example (outside systems that respond to pH) of a *well-defined chemically driven reversible valence tautomerization*. These results provide motivation for the future design of valence tautomers that respond to chemical stimuli.

To gain further insight we performed density functional theory (DFT) calculations¹⁷ on a simplified $[(\text{H}_8\text{Cz})\text{Mn}(\text{O})-\text{Zn}^{2+}]$ model where the eight TBP groups were replaced by H-atoms. Full geometry optimizations of the structures were done in a dielectric constant of $\epsilon = 5.7$. The optimized geometry for $[(\text{H}_8\text{Cz})\text{Mn}(\text{O})-\text{Zn}^{2+}]$ (Figure 3) has close-lying triplet and

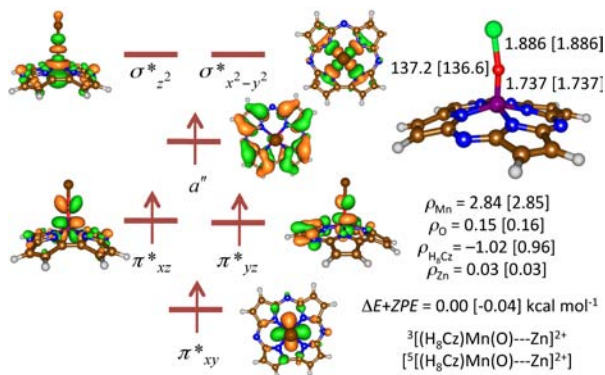


Figure 3. Frontier molecular orbitals and optimized geometries of $^{3,5}[(\text{H}_8\text{Cz})\text{Mn}^{\text{IV}}(\text{O})-\text{Zn}^{2+}]$ in a dielectric constant of $\epsilon = 5.7$. Bond lengths in Å, angles in deg, and spin densities (ρ) in au.

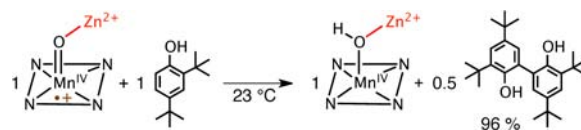
quintet spin states with $\pi_{xy}^* \pi_{xz}^* \pi_{yz}^* a^1$ occupation, where the H_8Cz π -orbital is either antiferromagnetically or ferromagnetically coupled to the unpaired electrons on the manganese. This configuration resembles the electronic state of Compound I of cytochrome P450, where metal-based π^* orbitals couple to a porphyrin radical.¹⁸ The Mn–O bond distance of 1.737 Å is considerably elongated compared to the triple bond in $(\text{TBP}_8\text{Cz})\text{Mn}^{\text{V}}(\text{O})$ (1.56 Å),¹³ while the Zn–O bond is rather short (1.886 Å) and implies significant bonding character between the two atoms. For comparison, an oxo-bridged $\text{Zn}^{2+}-\text{O}-\text{Zn}^{2+}$ complex shows Zn–O = 1.854(1) Å.¹⁹ Thus, the DFT-optimized structure predicts a tight bonding interaction between Mn(O) and Zn^{2+} , providing a theoretical underpinning for the large K_a value. This result is similar to that seen

for a non-heme $\text{Fe}(\text{O})-\text{Sc}^{3+}$ complex, which exhibits elongated Fe–O and short $\text{Sc}^{3+}-\text{O}$ bonds.^{7a}

The frontier molecular orbitals for the close-lying triplet and quintet states are shown in Figure 3. The lengthening of the Mn–O distance and disruption of the π donor ability of the oxo ligand bring the vacant $\pi^*(\text{Mn}-\text{O})$ orbitals down in energy (Table S5), allowing for an electron to be transferred from the Cz-based a^1 orbital into the vacant π_{yz}^* molecular orbital to give an Mn^{IV} center. At the same time, one of the π_{xy}^* electrons is promoted to π_{xz}^* giving an $S = 3/2$ spin state on Mn^{IV} coupled to an $S = 1/2$ spin state on H_8Cz . DFT calculations on the alternative $[(\text{H}_8\text{Cz})\text{Mn}^{\text{V}}(\text{O})-\text{Zn}^{2+}]$ singlet state locate it at $\Delta E + \text{ZPE} = 24.6 \text{ kcal mol}^{-1}$ above the triplet spin ground state. Overall, the DFT calculations are in excellent agreement with the conclusion that binding of Zn^{2+} causes interconversion to the valence tautomer $[(\text{TBP}_8\text{Cz})\text{Mn}^{\text{IV}}(\text{O})-\text{Zn}^{2+}]$.

Preliminary examination of the reactivity of the Mn–oxo complex in the presence of Zn^{2+} with substituted phenol substrates reveals a significant influence of the Zn^{2+} ion on HAT. Treatment of $(\text{TBP}_8\text{Cz})\text{Mn}^{\text{V}}(\text{O}):\text{Zn}(\text{OTf})_2$ (1:1) with 2,4-di-*tert*-butylphenol (5.0 equiv) at 23 °C led to the formation of $[(\text{TBP}_8\text{Cz})\text{Mn}^{\text{IV}}]^+$, as indicated by UV–vis. Product analysis by GC–FID showed the production of bis(phenol) dimer in high yield (96%) according to the stoichiometry in Scheme 4, with unreacted phenol accounting

Scheme 4



for the mass balance. This result is in agreement with the ET reactivity involving Fc, where $[(\text{TBP}_8\text{Cz})\text{Mn}^{\text{IV}}(\text{O})-\text{Zn}^{2+}]$ acts as a one-electron oxidant. In contrast, $(\text{TBP}_8\text{Cz})\text{Mn}^{\text{V}}(\text{O})$ functions only as a two-electron oxidant toward both phenols²⁰ and C–H substrates.²¹ Interestingly, our results are opposite to those found for $[(\text{TMC})\text{Fe}^{\text{IV}}(\text{O})]^{2+}$, for which it was shown that binding of Ca^{2+} and Sc^{3+} led to a two-electron reduction by Cp_2Fe as opposed to a one-electron process in the absence of redox-inactive metals.^{7a}

Reaction rates were measured for the reaction of $[(\text{TBP}_8\text{Cz})\text{Mn}^{\text{IV}}(\text{O})-\text{Zn}^{2+}]$ with excess 2,4,6-tri-*tert*-butylphenol, and the resulting k_{obs} values correlated linearly with substrate concentration (Figure 4). A second-order rate constant of $k'' = 0.25 \pm 0.02 \text{ M}^{-1} \text{ s}^{-1}$ was obtained, whereas

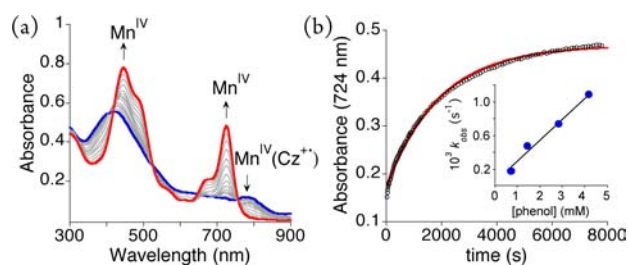


Figure 4. (a) Time-resolved UV–vis spectra of $[(\text{TBP}_8\text{Cz})\text{Mn}^{\text{IV}}(\text{O})-\text{Zn}^{2+}] + 2,4,6\text{-tri-}t\text{-butylphenol}$ (100 equiv) at 23 °C. (b) Change in absorbance at 724 nm vs time corresponding to the formation of $[(\text{TBP}_8\text{Cz})\text{Mn}^{\text{IV}}]^+$ (black circles) and best fit (red line). Inset: second-order rate plot.

in the absence of Zn^{2+} , $k'' = 0.074 \pm 0.007 \text{ M}^{-1} \text{ s}^{-1}$ for the same substrate.²⁰ Thus there is a modest rate enhancement of ~3-fold in the presence of the Zn^{2+} ion. Although this rate enhancement is not dramatic, it may be caused by the stabilization of the exchange-enhanced triplet state in $[(\text{TBP}_8\text{Cz}^{\bullet})\text{Mn}^{\text{IV}}(\text{O})-\text{Zn}^{2+}]$. Early work on the reactivity of non-heme iron(IV)-oxo complexes pointed to exchange-enhanced reactivity whereby high-spin states react faster than low-spin states.²² Also, the nature of the Lewis acid and substrates employed may play a key role in determining the overall effect on reaction rates.

In conclusion, we have described the first examination of the influence of a Lewis acid on the properties and reactivity of a high-valent Mn-oxo porphyrinoid complex. We also have demonstrated the first example of a chemically driven, reversible valence tautomerization between a metal ion and a redox-active ligand. The influence of the Lewis acidic Zn^{2+} on the $\text{Mn}^{\text{V}}(\text{O})$ complex is analogous to the effect of H^+ on His-ligated ferryl heme as shown by Gray and co-workers, where protonation of the terminal oxo ligand causes an intramolecular electron transfer to give a ferric porphyrin π -cation-radical.^{16d} In contrast, protonation of the ferryl intermediate (Compound II) in Cytochrome P450 (Cyt-P450) does not result in a conversion to the $\text{Fe}^{\text{III}} \pi$ -cation-radical but rather leaves the high-valent Fe^{IV} state intact.²³ The Cz ligand has a high propensity for stabilizing high-valent states but cannot maintain the Mn^{V} state upon metalation of the oxo donor. Thus our results, together with the influence of H^+ on His-ligated ferryl hemes, suggest that the strong donation from the unique thiolate ligand in Cyt-P450 may play an important role in stabilizing the high-valent metal ion in Compound II.

■ ASSOCIATED CONTENT

● Supporting Information

Experimental details, spectroscopic data, and computational details. This material is available free of charge via the Internet at <http://pubs.acs.org>.

■ AUTHOR INFORMATION

Corresponding Author

dpg@jhu.edu; sam.devisser@manchester.ac.uk

Present Address

[§]Department of Chemistry, Tufts University, 62 Talbot Avenue, Medford MA, 02155, USA

Notes

The authors declare no competing financial interest.

■ ACKNOWLEDGMENTS

This work was supported by the NSF (CHE0909587) to D.P.G. P.L. is grateful for the Queen Sirikit Scholarship (Thailand). S.P.d.V. thanks the National Service of Computational Chemistry Software (NSCCS) for CPU time.

■ REFERENCES

- (1) Umena, Y.; Kawakami, K.; Shen, J. R.; Kamiya, N. *Nature* **2011**, *473*, 55.
- (2) (a) McEvoy, J. P.; Brudvig, G. W. *Chem. Rev.* **2006**, *106*, 4455. (b) Sproviero, E. M.; Gascon, J. A.; McEvoy, J. P.; Brudvig, G. W.; Batista, V. S. *J. Am. Chem. Soc.* **2008**, *130*, 3428. (c) Siegbahn, P. E. M. *Acc. Chem. Res.* **2009**, *42*, 1871.
- (3) Miller, C. G.; Gordon-Wylie, S. W.; Horwitz, C. P.; Strazisar, S. A.; Peraino, D. K.; Clark, G. R.; Weintraub, S. T.; Collins, T. J. *J. Am. Chem. Soc.* **1998**, *120*, 11540.

- (4) (a) Lau, T. C.; Wu, Z. B.; Bai, Z. L.; Mak, C. K. *J. Chem. Soc., Dalton Trans.* **1995**, 695. (b) Lam, W. W. Y.; Yiu, S. M.; Lee, J. M. N.; Yau, S. K. Y.; Kwong, H. K.; Lau, T. C.; Liu, D.; Lin, Z. Y. *J. Am. Chem. Soc.* **2006**, *128*, 2851.

- (5) (a) Lai, S.; Lee, D. G. *Tetrahedron* **2002**, *58*, 9879. (b) Xie, N.; Binstead, R. A.; Block, E.; Chandler, W. D.; Lee, D. G.; Meyer, T. J.; Thiruvazhi, M. *J. Org. Chem.* **2000**, *65*, 1008.

- (6) Park, Y. J.; Ziller, J. W.; Borovik, A. S. *J. Am. Chem. Soc.* **2011**, *133*, 9258.

- (7) (a) Fukuzumi, S.; Morimoto, Y.; Kotani, H.; Naumov, P.; Lee, Y. M.; Nam, W. *Nature Chem.* **2010**, *2*, 756. (b) Morimoto, Y.; Kotani, H.; Park, J.; Lee, Y.-M.; Nam, W.; Fukuzumi, S. *J. Am. Chem. Soc.* **2010**, *133*, 403. (c) Park, J.; Morimoto, Y.; Lee, Y. M.; Nam, W.; Fukuzumi, S. *J. Am. Chem. Soc.* **2011**, *133*, 5236. (d) Park, J.; Morimoto, Y.; Lee, Y. M.; You, Y.; Nam, W.; Fukuzumi, S. *Inorg. Chem.* **2011**, *50*, 11612.

- (8) Egorova, O. A.; Tsay, O. G.; Khatua, S.; Meka, B.; Maiti, N.; Kim, M. K.; Kwon, S. J.; Huh, J. O.; Bucella, D.; Kang, S. O.; Kwak, J.; Churchill, D. G. *Inorg. Chem.* **2010**, *49*, 502.

- (9) (a) Simkhovich, L.; Mahammed, A.; Goldberg, I.; Gross, Z. *Chem.—Eur. J.* **2001**, *7*, 1041. (b) Meier-Callahan, A. E.; Di Bilio, A. J.; Simkhovich, L.; Mahammed, A.; Goldberg, I.; Gray, H. B.; Gross, Z. *Inorg. Chem.* **2001**, *40*, 6788.

- (10) Prokop, K. A.; Neu, H. M.; de Visser, S. P.; Goldberg, D. P. *J. Am. Chem. Soc.* **2011**, *133*, 15874.

- (11) (a) Weiss, R.; Bulach, V.; Gold, A.; Terner, J.; Trautwein, A. X. *J. Biol. Inorg. Chem.* **2001**, *6*, 831. (b) Evangelio, E.; Ruiz-Molina, D. *Eur. J. Inorg. Chem.* **2005**, 2957. (c) Pan, Z. Z.; Harischandra, D. N.; Newcomb, M. *J. Inorg. Biochem.* **2009**, *103*, 174. (d) Spreer, L. O.; Maliyackel, A. C.; Holbrook, S.; Otvos, J. W.; Calvin, M. *J. Am. Chem. Soc.* **1986**, *108*, 1949. (e) Groves, J. T.; Quinn, R.; McMurry, T. J.; Lang, G.; Boso, B. *Chem. Commun.* **1984**, 1455.

- (12) Kaustov, L.; Tal, M. E.; Shames, A. I.; Gross, Z. *Inorg. Chem.* **1997**, *36*, 3503.

- (13) Lansky, D. E.; Mandimutsira, B.; Ramdhanie, B.; Clausén, M.; Penner-Hahn, J.; Zvyagin, S. A.; Telser, J.; Krzystek, J.; Zhan, R. Q.; Ou, Z. P.; Kadish, K. M.; Zakharov, L.; Rheingold, A. L.; Goldberg, D. P. *Inorg. Chem.* **2005**, *44*, 4485.

- (14) Fukuzumi, S.; Kotani, H.; Prokop, K. A.; Goldberg, D. P. *J. Am. Chem. Soc.* **2011**, *133*, 1859.

- (15) Kurahashi, T.; Kikuchi, A.; Tosha, T.; Shiro, Y.; Kitagawa, T.; Fujii, H. *Inorg. Chem.* **2008**, *47*, 1674.

- (16) (a) Kundu, N.; Maity, M.; Chatterjee, P. B.; Teat, S. J.; Endo, A.; Chaudhury, M. *J. Am. Chem. Soc.* **2011**, *133*, 20104. (b) Storr, T.; Verma, P.; Pratt, R. C.; Wasinger, E. C.; Shimazaki, Y.; Stack, T. D. P. *J. Am. Chem. Soc.* **2008**, *130*, 15448. (c) Pratt, R. C.; Lyons, C. T.; Wasinger, E. C.; Stack, T. D. *J. Am. Chem. Soc.* **2012**, *134*, 7367. (d) Low, D. W.; Winkler, J. R.; Gray, H. B. *J. Am. Chem. Soc.* **1996**, *118*, 117.

- (17) (a) de Visser, S. P. *J. Am. Chem. Soc.* **2010**, *132*, 1087. (b) Kumar, D.; Thiel, W.; de Visser, S. P. *J. Am. Chem. Soc.* **2011**, *133*, 3869.

- (18) (a) Green, M. T. *J. Am. Chem. Soc.* **1999**, *121*, 7939. (b) de Visser, S. P.; Shaik, S.; Sharma, P. K.; Kumar, D.; Thiel, W. *J. Am. Chem. Soc.* **2003**, *125*, 15779.

- (19) Ruf, M.; Vahrenkamp, H. *Inorg. Chem.* **1996**, *35*, 6571.

- (20) Lansky, D. E.; Goldberg, D. P. *Inorg. Chem.* **2006**, *45*, 5119.

- (21) Prokop, K. A.; de Visser, S. P.; Goldberg, D. P. *Angew. Chem., Int. Ed.* **2010**, *49*, 5091.

- (22) (a) de Visser, S. P. *J. Am. Chem. Soc.* **2006**, *128*, 15809. (b) Shaik, S.; Chen, H.; Janardanan, D. *Nature Chem.* **2011**, *3*, 19.

- (23) Behan, R. K.; Hoffart, L. M.; Stone, K. L.; Krebs, C.; Green, M. T. *J. Am. Chem. Soc.* **2006**, *128*, 11471–11474.